Solar Energy Materials and Solar Cells 192 (2019) 134–139

Contents lists available at ScienceDirect

Solar Energy Materials and Solar Cells

journal homepage: www.elsevier.com/locate/solmat

Low-temperature dark anneal as pre-treatment for LeTID in multicrystalline silicon

Marko Yli-Koski, Michael Serué, Chiara Modanese, Henri Vahlman, Hele Savin*

Aalto University, Department of Electronics and Nanoengineering, Tietotie 3, Espoo, Finland

ARTICLE INFO

Keywords:
LeTID
Multicrystalline silicon
Copper in silicon
Precipitation
PERC
Minority-carrier lifetime

ABSTRACT

Light and elevated temperature induced degradation (LeTID) is currently a severe issue in crystalline silicon photovoltaics, which has led to numerous efforts to both understand the mechanism and to mitigate it. Here we show that a low-temperature dark anneal performed as the last step in typical solar cell processing influences greatly LeTID characteristics, both the strength of the degradation and the degradation kinetics. While a relatively short anneal in the temperature range of 200–240 °C can be detrimental to LeTID by doubling the degradation intensity, an optimized anneal at 300 °C shows the opposite trend providing an efficient means to eliminate LeTID. Furthermore, we show that the simulated recombination activity of metal precipitation and dissolution during the dark anneal correlates with the experiments, suggesting a possible explanation for the LeTID mechanism.

1. Introduction

Light induced degradation (LID) in industrial p-type Czochralski (CZ) silicon has been studied extensively in the past and it is often referred to as BO-LID due to involvement of boron and oxygen in the defect formation [1]. Recently, a new type of degradation called Light and elevated Temperature-Induced Degradation (LeTID), has been observed, especially in p-type Passivated Emitter and Rear Cell (PERC) architectures, and it has been shown to be more severe than BO-LID [2]. Although LeTID was originally observed in multicrystalline silicon (mc-Si) PERC cells, it has later been shown to appear also in CZ [3] and even in FloatZone silicon [4]. In addition to solar cells, LeTID shows characteristic degradation also in minority carrier lifetime and so-called implied-V_{oc} samples [5].

While LeTID is clearly affected by charge-carrier injection (*e.g.* by light), it is also affected by thermal treatments, especially by the contact firing process [6–9]. In addition, recent studies have reported the influence of low-temperature dark anneal (75–275 °C) on LeTID [8,10,11]. More specifically, it has been shown that a dark anneal (hereinafter abbreviated as DA) alone can induce degradation and regeneration similar to LeTID [8,11,12] and that degradation kinetics and strength depend on the DA temperature [8]. Low-temperature DA as a pre-treatment to LeTID has only been studied in temperatures below 275 °C and so far only negative impact on LeTID has been reported [7,8,11–13]. The only exception to this behavior was reported by Sharma et al., who noticed reduced LeTID after 20 min of DA at 550 °C [14].

This work studies the impact of relatively long low-temperature dark anneal on LeTID in order to gain further insight into the currently unknown defect mechanism, although strong evidence has been reported for hydrogen playing a crucial role [15]. Our hypothesis is that a long anneal at slightly higher temperature than 275 °C may have a significant contribution to the diffusion of the defects. We are especially interested if the degradation and regeneration during DA resemble metal precipitation kinetics, since earlier studies indicate that some metals may still be present in the bulk after the last high temperature step [9,16–19]. Further, we are interested to study whether the DA can influence the recombination activity of LeTID and possibly mitigate it. To answer these questions we perform LeTID experiments in mc-Si pre-treated with DA at various temperatures (200–300 °C) and durations (0.5–44 h). The maximum temperature is limited to 300 °C in order to be able to extend the results to finished cells. To explain the results we apply copper precipitation model [20] and compare the simulations with the experimental results.

2. Experimental

In this work we used commercial square 156 × 156 mm^2 B-doped high-performance mc-Si wafers. The wafers had resistivity of 1.3 Ωcm and thickness of 190 μm and they were all taken from the same height

* Corresponding author
E-mail address: hele.savin@aalto.fi (H. Savin).

https://doi.org/10.1016/j.solmat.2018.12.021
Received 4 September 2018; Received in revised form 24 October 2018; Accepted 11 December 2018
Available online 27 December 2018

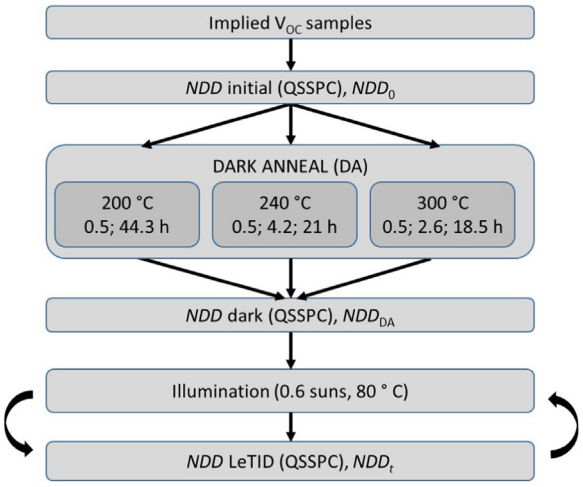

Fig. 1. Process sequence of the studied implied V_{OC} samples. The NDD was continuously measured during the illumination time. The reference sample (*i.e.* no DA after firing) is not included in the figure.

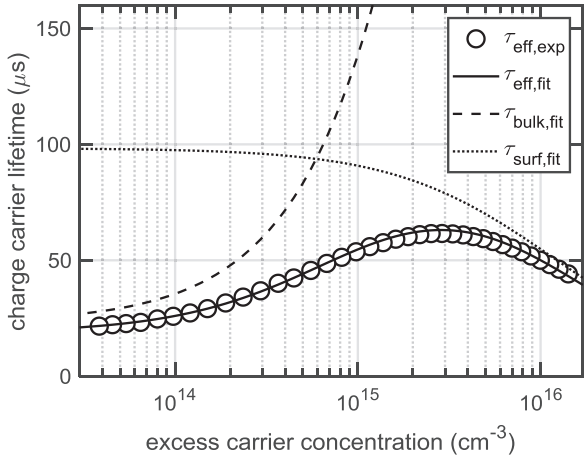

Fig. 2. Charge carrier lifetime *vs* excess carrier concentration. The symbols represent measured effective lifetime values. Dashed and dotted lines are fitted bulk and surface lifetime values that are used to calculate the total effective lifetime values (solid line). Intrinsic lifetime values are also included in the fitting, but their values are not shown because they are above 1 ms. The fitted bulk and surface lifetimes are 153 µs and 90 µs at excess carrier concentration of 1.1e15 cm^{-3}. The experimental data is taken from the sample dark annealed at 300 °C for 2.6 h and illuminated for 3.6 h.

of the ingot. The wafers were processed at industrial pilot line, following industrial standard processing parameters for PERC to form so-called implied-V_{oc} ($ImpV_{oc}$) samples. On the front side, the samples had a $POCl_3$ diffused n^+ emitter with sheet resistance of ~110 Ωcm that was passivated with plasma-enhanced chemical vapour deposited (PECVD) SiN_X, while the backside was passivated with a typical PECVD AlO_X/SiN_X stack. The last processing step was a few seconds of firing at T_{peak} = 835 °C to activate LeTID.

Nine squares were cut from each wafer after processing. The initial lifetime was mapped to check that the wafers had uniform quality. The initial bulk lifetime (with the injection level of 1.1e15 cm^{-3}) in each sample was measured to be 490 ± 70 µs. The samples were then annealed in dark at different combinations of temperature and time (see Fig. 1), while one sample remained as a reference (*i.e.,* it did not experience any DA after firing). The wafers were then exposed to degradation conditions, which consisted of illumination at 0.6 suns in 80 °C for a total of ~1000 h. The light source was an LED lamp, with the illumination spectrum predominantly in the range 400–800 nm and peaking at 550 nm. Note that in the beginning of illumination the intensity was reduced to 0.1 suns for 1.5 h to check that the defect formation has similar dependency on the illumination intensity before and after the DA. Some samples were used for studying the kinetics of the defect formation during the DA. The recombination rate needed to be measured at room temperature and we wanted to avoid the influence of repeated cooling and heating of the sample. Therefore, instead of annealing one sample for multiple times, identical samples were used for DA experiments with various times to get reliable time dependent DA curves.

The effective minority carrier lifetimes were measured both before and after DA. The evolution of the lifetime was sequentially monitored also during the illumination. The lifetimes as a function of excess carrier density were measured using a quasi-steady-state photoconductance (QSS-PC) tool (Sinton Instruments WCT-120TS) at 24 ± 1 °C. Since LeTID is known to be a bulk degradation phenomenon and surface degradation has been observed both during DA [21] and illumination [22–25], the bulk and surface recombination components should be carefully separated when analyzing the measured data. This was done by fitting to the measured injection-dependent lifetime the emitter saturation current density, J_{0e} (surface) and charge carrier lifetime, τ_{bulk} (bulk) components, as described in Ref. [26]. Auger and radiative recombination at the emitter was modeled according to [27,28], and the rear surface recombination was included in J_{0e}. Shockley-Read-Hall (SRH) single defect-level model with energy level of $E_c - 0.35$ eV and capture cross-section ratio of k = 66.4 were used to calculate τ_{bulk}. The same parameters were used for the dark annealed and illuminated samples. The sample that was dark annealed at 300 °C for 18.5 h had higher bulk lifetime after DA than the other samples and thus slightly different defect parameters were used ($E_c - 0.32$ eV and k = 44.5) to reduce the noise to obtain more reliable τ_{bulk}. The chosen SRH parameters resulted in the lowest fitting error, but we checked that using LeTID related defect parameters from literature ($E_c - 0.56$ eV and k = 33.4) [8], the extracted bulk lifetime values were comparable. The normalized defect densities that are presented later in this article were calculated using the above single-defect level SRH bulk lifetime values at an excess carrier concentration of 1.1·15 cm^{-3} ($0.1 \cdot N_a$).

An example of the injection dependent recombination measurement and related τ_{bulk} and J_{0e} extraction is shown in Fig. 2. The figure shows that the model fits well the measurement data resulting in low fitting error when extracting the bulk lifetime. The fitting error did not increase during illumination.

The normalized defect density (*NDD*) as a function of illumination time was determined with the following equation:

$$NDD_t = \frac{1}{\tau_{bulk}(t)} - \frac{1}{\tau_{bulk,DA}} \quad (1)$$

where τ_{bulk} is, as described above, the bulk lifetime extracted from the measurement data with the SRH single-defect level model during illumination and $\tau_{bulk,DA}$ is the bulk lifetime after dark annealing (before illumination). The normalized defect densities after dark anneal, after 1000 h illumination and at maximum degradation were calculated with the following equations

$$NDD_{DA} = \frac{1}{\tau_{bulk,DA}} - \frac{1}{\tau_{bulk,0}} \quad (2)$$

$$NDD_{1000h} = \frac{1}{\tau_{bulk,1000h}} - \frac{1}{\tau_{bulk,0}} \quad (3)$$

$$NDD_{max.deg} = \frac{1}{\tau_{bulk,max.deg}} - \frac{1}{\tau_{bulk,DA}} \quad (4)$$

where $\tau_{bulk,0}$, $\tau_{bulk,1000h}$ and $\tau_{bulk,max.deg}$ are the bulk lifetimes before dark annealing (initial) and after 1000 h illumination and at maximum degradation, respectively. The change in the maximum normalized defect density ($NDD_{max.deg,change}$) was calculated with the following equation

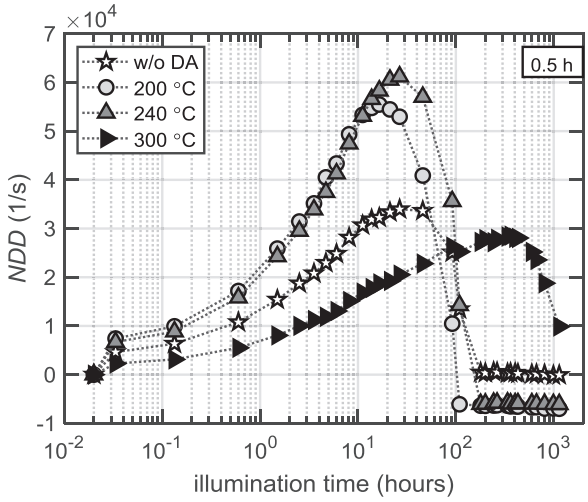

Fig. 3. Normalized defect density (NDD) *vs* illumination time (0.6 suns, 75 °C) in the samples dark annealed at 200 °C (circle), 240 °C (grey up-pointing triangle) and 300 °C (black right-pointing triangle) for 0.5 h prior to illumination. The sample without dark anneal (DA) is also shown as a reference (stars). The symbols are the measured values and the dashed lines serve as guide to the eye. The legend shows the DA temperature. The normalization is done with the values measured directly after the DA (*i.e.* NDD_{DA}, values before illumination).

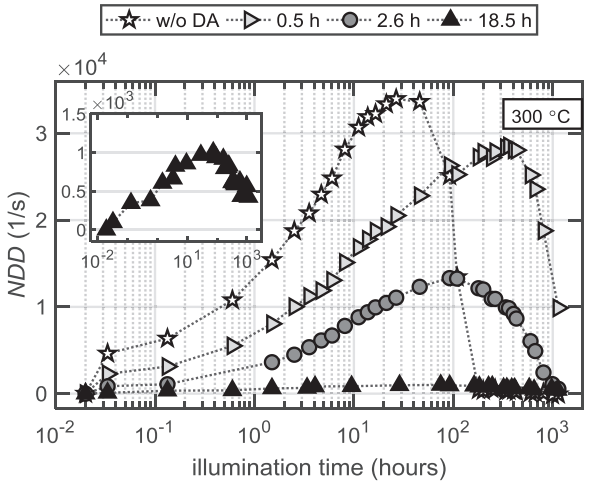

Fig. 4. Normalized defect density (NDD) *vs* illumination time (0.6 suns, 75 °C) in the samples dark annealed at 300 °C for 0.5 h (right-pointing triangle), 2.6 h (grey circle) and 18.5 h (black up-pointing triangle) prior to illumination. The reference sample without dark anneal (DA) is also shown as a reference (stars). The symbols are the measured values and the dashed lines serve as guide to the eye. The legend shows the DA times. The inset zooms on the sample annealed for 18.5 h. Normalization is done with the values measured directly after the DA (*i.e.* NDD_{DA}, values before illumination).

$$NDD_{\mathrm{max.deg.change}} = 100\%*(NDD_{\mathrm{max.deg}} - NDD_{\mathrm{max.deg,ref}})/NDD_{\mathrm{max.deg,ref}} \quad (5)$$

where $NDD_{\mathrm{max.deg,ref}}$ is the value for the reference sample without dark annealing and it was calculated with Eq. (4) using $\tau_{\mathrm{bulk},0}$ instead of $\tau_{\mathrm{bulk,DA}}$.

NDD has a direct correlation to the intensity of cell degradation. For instance in an industrial 20% mc-Si PERC cells, a typical maximum NDD is in the order of 10^5 1/s in lifetime samples after light degradation, which corresponds the absolute cell efficiency degradation of 2% [29]. By reducing NDD ~50%, the corresponding absolute degradation would be only ~1%.

3. Results

3.1. Impact of dark annealing temperature on LeTID

Fig. 3 shows the normalized defect density (NDD_t) as a function of illumination time at elevated temperature (*i.e.* LeTID curve) in the samples that were exposed to 0.5 h dark anneal (DA) at various temperatures prior to illumination. The reference sample without any anneal is also shown in the figure. The LeTID curve measured in the reference sample is in close agreement with literature [12]. However, the DA temperature seems to have a large impact on LeTID behavior in regards to both the kinetics and the maximum degradation and regeneration. If the dark anneal temperature is below 300 °C, the maximum degradation is obtained slightly faster as compared to the reference sample, *i.e.* after 15–25 h or 35 h of illumination, respectively. Furthermore, the measured maximum NDD is much higher, even doubled, after such anneals. Interestingly, when increasing the dark anneal temperature to 300 °C, LeTID slows down considerably and the maximum LeTID is reached only after 400 h. Furthermore, the maximum NDD is slightly lower than in the reference sample, suggesting that 300 °C and possibly higher temperatures could be beneficial in reducing LeTID.

Additionally, it is interesting to see that after the regeneration and saturation, the final *NDD* becomes negative as compared to the initial value measured after the DA (NDD_{DA}), which is especially clear in the 200 °C and 240 °C samples. The phenomenon suggests that some defects are possibly generated during the DA and are then consequently regenerated during the following illumination. Indeed, the DA itself slightly increased the initial *NDD*, *i.e.* $NDD_{DA} > NDD_0$. Similar regeneration of DA-induced defects during illumination is also observed in Refs. [10,11]. This phenomenon is further clarified in Section 3.3, where the time dependence of the DA defect generation is presented.

3.2. Impact of dark annealing time on LeTID

Since the 300 °C anneal showed the most interesting characteristics, we extended the anneal times to see if the duration has any impact on LeTID. Thus, Fig. 4 shows the same LeTID curve presented in Fig. 3, but with varying DA times. Indeed, it is seen that both the maximum LeTID and the timescale of degradation depends heavily on the anneal time, *i.e.* LeTID is stronger the shorter the DA duration. Interestingly, after very long DA (18.5 h), during following illumination LeTID is almost totally suppressed. If NDD_t is normalized to NDD_{DA}, in the sample with 18.5 h DA, the NDD_t is positive during the whole duration of the illumination (see inset in Fig. 4). However, if NDD is normalized to the value measured prior to dark anneal (NDD_0), NDD_t remains negative during the whole duration of the illumination. This means that such DA has increased the initial bulk lifetime, and additionally, during all points of illumination, the bulk lifetime remains above the initial value of the standard reference cell that has not experienced such DA.

In light of such promising results, the longer dark anneals were also performed at lower temperatures, to see if a similar mechanism is present there too. The results of these experiments are summarized in Table 1. Indeed, the long anneals at lower temperatures show the same trend and a clear correlation of annealing time on the reduced LeTID. Obviously the required time is much longer for LeTID mitigation at lower temperatures. At 200 °C and 240 °C, the required time to reduce LeTID is 44 and 21 h, respectively. Total LeTID suppression at 200 °C and 240 °C would thus likely take much longer duration and they would become impractical.

While long dark anneals as those summarized in Table 1 have not been reported before as pre-treatment for LeTID, there are some studies showing the impact of short low-temperature DA on LeTID characteristics. When DA was performed at temperatures and times in the range 125–232 °C and 8 min–2.5 h, respectively, it always resulted in increased LeTID and it also fastened the degradation [7,11–13]. This

Table 1
List of the samples with respective dark anneal (DA) temperature, time and the corresponding defect densities at various stages of degradation. The defect density after DA (NDD_{DA}) and after 1000 h illumination (NDD_{1000h}), were calculated with Eqs. (2) and (3), respectively. The strength of the degradation ($NDD_{max.deg.change}$) as compared to the non-annealed reference sample was calculated with Eq. (5). Positive (negative) value means that the maximum LeTID is higher (lower) than in the reference sample without DA.

DA temp. (°C)	DA time (h)	NDD_{DA} (1/s)	NDD_{1000h} (1/s)	$NDD_{max.deg\ change}$ (%)
200	0.5	6800	−200	63
200	44.3	1100	0	−55
240	0.5	5600	−500	80
240	4.2	900	−500	15
240	21	−800	−900	−60
300	0.5	−700	9200	−16
300	2.6	−1300	−700	−61
300	18.5	−1100	−700	−97

result is in line with our samples dark annealed at 200 °C and 240 °C (Fig. 3). When DA was performed at 250–275 °C [12] or at 300 °C [14], LeTID became extremely slow and no regeneration was reported, even after 1000 h illumination [12]. This behavior is similar to our sample dark annealed at 300 °C for 0.5 h, although in our study the regeneration started after 400 h. When the DA temperature was increased to 550 °C, LeTID kinetics became faster [14]. At these higher temperatures, 20 min DA at both 300 °C and 550 °C resulted in the reduction of LeTID, with a more pronounced effect at 550 °C [14]. Thus, combining those results and ours, it can be speculated that a long anneal at 550 °C could also mitigate LeTID, although a relatively higher temperature may change again the precondition for LeTID defects.

The contact firing step during cell processing can be also considered as a dark anneal pre-treatment, although it has typically a rather short duration (tens of seconds) and it is also performed at high temperatures ($T_{PEAK} > 600$ °C). Nonetheless, the firing parameters have shown to impact LeTID, *e.g.* a slow cooling [30] or a low peak temperature ($\leq$675 °C) [7,8] drastically reduce LeTID. In addition, it was shown that, in case of multiple firing steps, the degradation intensity and kinetics depend on the last step [7]. In all the implied V_{OC} and solar cell samples reported in literature until now, LeTID has been clearly present when firing temperature has been 700 °C or above. However, the general trend reported in literature is similar to what observed in our samples, *i.e.* DA at temperatures $\leq$675 °C reduces LeTID. These short firing anneals are still difficult to compare with our results, since we have shown that the time of the DA has also a significant impact on the subsequent LeTID behavior. This is further clarified in the following section.

3.3. Time-evolution of recombination during dark anneal

Based on the experimental results reported above, the DA affects the defects that are responsible for LeTID, and it is therefore crucial to understand the phenomena occurring during the DA. To obtain further insight into this, we studied the evolution of the recombination rate during the DA, at the same temperatures used in the experiments (*i.e.* 200 °C, 240 °C and 300 °C, as shown in Fig. 5a–c, respectively).

The general trend observed in Fig. 5 is that the recombination rate strongly increases in the beginning of DA and then decreases back to the initial value – or even below. A similar behavior was reported also in earlier studies at temperatures of 175 °C (in implied V_{oc} samples) [8] and 250 °C (in V_{oc} of finished cells) [12]. Such behavior resembles the actual LeTID characteristics and indeed, it has been suggested earlier that the defects generated during DA are the same that are generated during LeTID. The speculations have recently been confirmed by injection dependent lifetime spectroscopy (IDLS) analysis [8]. From the LeTID point of view, it would be beneficial to have as low defect density as possible prior to illumination. Thus, the results shown in the Fig. 5 suggest that the longer the DA anneal time and the higher the temperature, the closer to optimal the initial conditions are (*i.e.* prior to illumination). Indeed, this was also confirmed by our experiments (as shown in Figs. 3 and 4).

There are currently many speculations about the root cause of the LeTID defect and how to explain the similar DA recombination activity. The majority of both theories and experiments support the presence of hydrogen as one crucial component and rules out the role of metal contamination [15], while other studies support the involvement of fast diffusing metals [18,31]. In this work we study the latter approach, *i.e.* the possibility of formation and dissolution of recombination active metal precipitates and the simultaneous segregation of the mobile metals to the surface or the emitter. Modeling the metal precipitation and dissolution, as well as segregation and diffusion at different temperatures, is relatively straightforward based on the models found in literature [20]. Such models can be used for different impurities, but in this work we use the physical parameters for copper [32]. In addition to modeling the impurity redistributions, we also simulate the recombination rate during the dark anneals reported above to see if they correlate with the experiments. Regarding the defect formation, the model by Vahlman et al. [20] is used, which couples the kinetic precipitation model and the Schottky junction model, thus enabling the calculation of charge carrier recombination rate induced by precipitates. In the simulations the initial interstitial and precipitated copper concentrations in the bulk of the wafer were 2e13 cm^{-3} and 7e11 cm^{-3}, respectively. Note that copper concentration in the emitter remains below the solubility and thus the copper transport to the emitter is a fully diffusion limited process.

Fig. 5 shows that the simulations show a similar trend with the experiments. Since it is known that the model used for the defect formation overestimates the copper precipitation [32], the simulated values of the recombination rate are much higher than the measured values, especially at long annealing times. It is known that by adjusting the interfacial energy between precipitate and silicon matrix, a better agreement also at long annealing times would be reachable. Nevertheless, the trend is the same with all samples. The increase in the bulk recombination rate at the beginning of the dark anneal can be explained by the formation of recombination active precipitates, which occurs instantly after firing as the fast cooling leads to a strong supersaturation of dissolved metals. The maximum recombination rate is the highest at the lowest temperature (200 °C), because the driving force for precipitation decreases as a function of temperature. On the other hand, the regeneration of the defect after being annealed for some time can be explained by precipitate dissolution, *i.e.* the precipitates dissolve because the dissolved metal concentration decreases below the solid solubility due to segregation to emitter (or surfaces). The dissolution is the fastest at the highest temperature (300 °C) because the driving force for precipitation is the lowest. Therefore, the bulk recombination rate starts to decrease earlier when increasing temperature. It should be noticed that metal precipitate dissolution is a slow process, which explains the decreasing trend observed in the simulation even after 100 h of DA. To summarize, the change in the bulk recombination rate in our samples could be explained with fast metal precipitation and slow dissolution. Similar phenomenon could be also present under LeTID conditions, although the dissolution (*i.e.* regeneration) would be very slow due to low metal solubility close to room temperature.

4. Conclusions

In this contribution we have shown that a dark anneal performed prior to illumination has a large impact on LeTID behavior. Both the temperature and time of the anneal affect the maximum LeTID as well as the kinetics of degradation. The most interesting finding is that extending the dark anneal time to several hours suppresses LeTID, *i.e.* LeTID was removed almost completely at 300 °C. However, dark anneal for 0.5 h at 300 °C had a strong negative impact, as it slowed down

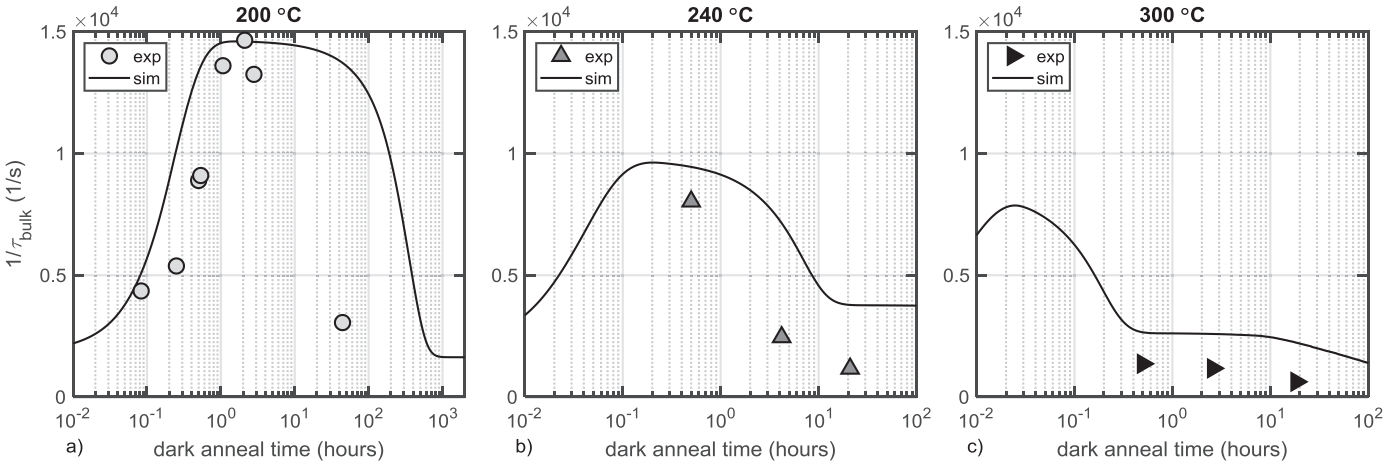

Fig. 5. Bulk recombination rate as a function of dark annealing time at a) T = 200 °C, b) T = 240 °C and c) T = 300 °C. The experimental recombination values (symbols) are compared to the simulated ones (lines). The samples went for LeTID aging after they experienced DA anneal in b) and c). The initial value for the recombination rate before DA in each sample was measured to be 0.21 ± 0.03e4 1/s.

greatly the LeTID degradation and regeneration rate (saturation was not reached even after 1000 h of illumination). Similarly, dark anneal at lower temperatures (≤250 °C) lead to much stronger LeTID compared to samples without any dark anneal. A possible theory for the defect formation mechanism during dark anneal was given based on simulations of metal precipitation and dissolution, which showed similar trends with the experiments. The next step will be to study the impact of such long anneals on LeTID in the finished PERC cells.

Acknowledgements

The work has been partially funded through the European Research Council under the European Union's FP7 Programme ERC (European Research Council) grant agreement no. 307315. The authors acknowledge the discussions with Dr. Antti Haarahiltunen.

References

[1] J. Lindroos, H. Savin, Review of light-induced degradation in crystalline silicon solar cells, Sol. Energy Mater. Sol. Cells 147 (2016) 115–126, https://doi.org/10.1016/j.solmat.2015.11.047.

[2] K. Ramspeck, S. Zimmermann, H. Nagel, A. Metz, Y. Gassenbauer, B. Birkmann, A. Seidl, Light induced degradation of rear passivated mc-Si solar cells, Proc. 27th Eur. Photovolt. Sol. Energy Conf. Exhib. (2012) 861–865.

[3] F. Fertig, R. Lantzsch, A. Mohr, M. Schaper, M. Bartzsch, D. Wissen, F. Kersten, A. Mette, S. Peters, A. Eidner, J. Cieslak, K. Duncker, M. Junghänel, E. Jarzembowski, M. Kauert, B. Faulwetter-Quandt, D. Meißner, B. Reiche, S. Geißler, S. Hörnlein, C. Klenke, L. Niebergall, A. Schönmann, A. Weihrauch, F. Stenzel, A. Hofmann, T. Rudolph, A. Schwabedissen, M. Gundermann, M. Fischer, J.W. Müller, D.J.W. Jeong, Mass production of p-type Cz silicon solar cells approaching average stable conversion efficiencies of 22%, Energy Procedia 124 (2017) 338–345, https://doi.org/10.1016/J.EGYPRO.2017.09.308.

[4] T. Niewelt, M. Selinger, N.E. Grant, W. Kwapil, J.D. Murphy, M.C. Schubert, Light-induced activation and deactivation of bulk defects in boron-doped float-zone silicon, J. Appl. Phys. 121 (2017), https://doi.org/10.1063/1.4983024.

[5] D. Bredemeier, D. Walter, S. Herlufsen, J. Schmidt, Lifetime degradation and regeneration in multicrystalline silicon under illumination at elevated temperature, AIP Adv. 6 (2016), https://doi.org/10.1063/1.4944839.

[6] K. Nakayashiki, J. Hofstetter, A.E. Morishige, T.T.A. Li, D.B. Needleman, M.A. Jensen, T. Buonassisi, Engineering solutions and root-cause analysis for light-induced degradation in p-type multicrystalline silicon PERC modules, IEEE J. Photovolt. 6 (2016) 860–868, https://doi.org/10.1109/JPHOTOV.2016.2556981.

[7] C.E. Chan, D.N.R. Payne, B.J. Hallam, M.D. Abbott, T.H. Fung, A.M. Wenham, B.S. Tjahjono, S.R. Wenham, Rapid stabilization of high-performance multicrystalline p-type silicon PERC cells, IEEE J. Photovolt. 6 (2016) 1473–1479, https://doi.org/10.1109/JPHOTOV.2016.2606704.

[8] D. Chen, M. Kim, B.V. Stefani, B.J. Hallam, M.D. Abbott, C.E. Chan, R. Chen, D.N.R. Payne, N. Nampalli, A. Ciesla, T.H. Fung, K. Kim, S.R. Wenham, Evidence of an identical firing-activated carrier-induced defect in monocrystalline and multicrystalline silicon, Sol. Energy Mater. Sol. Cells 172 (2017) 293–300, https://doi.org/10.1016/j.solmat.2017.08.003.

[9] R. Eberle, W. Kwapil, F. Schindler, S.W. Glunz, M.C. Schubert, Firing temperature profile impact on light induced degradation in multicrystalline silicon, Energy Procedia 124 (2017) 712–717, https://doi.org/10.1016/j.egypro.2017.09.082.

[10] T.H. Fung, M. Kim, D. Chen, C.E. Chan, B.J. Hallam, R. Chen, D.N.R. Payne, A. Ciesla, S.R. Wenham, M.D. Abbott, A four-state kinetic model for the carrier-induced degradation in multicrystalline silicon: introducing the reservoir state, Sol. Energy Mater. Sol. Cells 184 (2018) 48–56, https://doi.org/10.1016/j.solmat.2018.04.024.

[11] T. Luka, M. Turek, C. Hagendorf, Defect formation under high temperature dark-annealing compared to elevated temperature light soaking, Sol. Energy Mater. Sol. Cells 187 (2018) 194–198, https://doi.org/10.1016/j.solmat.2018.06.043.

[12] C. Chan, T.H. Fung, M. Abbott, D. Payne, A. Wenham, B. Hallam, R. Chen, S. Wenham, Modulation of carrier-induced defect kinetics in multi-crystalline silicon PERC cells through dark annealing, Sol. RRL 1 (2017) 1600028, https://doi.org/10.1002/solr.201600028.

[13] T.H. Fung, C.E. Chan, B.J. Hallam, D.N.R. Payne, M.D. Abbott, S.R. Wenham, Impact of annealing on the formation and mitigation of carrier-induced defects in multi-crystalline silicon, Energy Procedia 124 (2017) 726–733, https://doi.org/10.1016/j.egypro.2017.09.087.

[14] R. Sharma, A.G. Aberle, J.B. Li, Optimization of belt furnace anneal to reduce light and elevated temperature induced degradation of effective carrier lifetime of p-type multicrystalline silicon wafers, Sol. RRL 1800070 (2018) 1–8, https://doi.org/10.1002/solr.201800070.

[15] T. Niewelt, F. Schindler, W. Kwapil, R. Eberle, J. Schön, M.C. Schubert, Understanding the light-induced degradation at elevated temperatures: similarities between multicrystalline and floatzone p-type silicon, Prog. Photovolt. Res. Appl. 26 (2018) 533–542, https://doi.org/10.1002/pip.2954.

[16] T. Luka, M. Turek, S. Großer, C. Hagendorf, Microstructural identification of Cu in solar cells sensitive to light-induced degradation, Phys. Status Solidi Rapid Res. Lett. 11 (2017) 1600426, https://doi.org/10.1002/pssr.201600426.

[17] T. Luka, M. Turek, C. Kranert, S. Großer, C. Hagendorf, Microstructural investigation of LID sensitive mc-PERC solar cells, Energy Procedia 124 (2017) 759–766, https://doi.org/10.1016/j.egypro.2017.09.080.

[18] N. Nampalli, H.S. Laine, J. Colwell, V. Vähänissi, A. Inglese, C. Modanese, H. Vahlman, M. Yli-Koski, H. Savin, Rapid thermal anneal activates light induced degradation due to copper redistribution, Appl. Phys. Lett. 113 (2018) 032104, https://doi.org/10.1063/1.5029347.

[19] C. Modanese, M. Wagner, F. Wolny, A. Oehlke, H.S. Laine, A. Inglese, H. Vahlman, M. Yli-Koski, H. Savin, Impact of copper on light-induced degradation in Czochralski silicon PERC solar cells, Sol. Energy Mater. Sol. Cells 186 (2018) 373–377, https://doi.org/10.1002/pssa.201700321.

[20] H. Vahlman, A. Haarahiltunen, W. Kwapil, J. Schön, A. Inglese, H. Savin, Modeling of light-induced degradation due to Cu precipitation in p-type silicon. I. General theory of precipitation under carrier injection, J. Appl. Phys. 121 (2017), https://doi.org/10.1063/1.4983454.

[21] D. Sperber, A. Herguth, G. Hahn, Instability of dielectric surface passivation quality at elevated temperature and illumination, Energy Procedia 92 (2016) 211–217, https://doi.org/10.1016/j.egypro.2016.07.061.

[22] T. Niewelt, W. Kwapil, M. Selinger, A. Richter, M.C. Schubert, Long-term stability of aluminum oxide based surface passivation schemes under illumination at elevated temperatures, IEEE J. Photovolt. 7 (2017) 1197–1202, https://doi.org/10.1109/JPHOTOV.2017.2713411.

[23] D. Sperber, A. Graf, A. Heilemann, A. Herguth, G. Hahn, Bulk and surface instabilities in boron doped float-zone samples during light induced degradation treatments, Energy Procedia 124 (2017) 794–798, https://doi.org/10.1016/j.egypro.2017.09.349.

[24] D. Sperber, A. Graf, D. Skorka, A. Herguth, G. Hahn, Degradation of surface passivation on crystalline silicon and its impact on light-induced degradation experiments, IEEE J. Photovolt. 7 (2017) 1627–1634, https://doi.org/10.1109/JPHOTOV.2017.2755072.

[25] F. Kersten, J. Heitmann, J.W. Müller, Influence of Al2O3 and SiNx passivation layers on LeTID, Energy Procedia 92 (2016) 828–832, https://doi.org/10.1016/j.egypro.2016.07.079.
[26] A. Cuevas, D. Macdonald, Measuring and interpreting the lifetime of silicon wafers, Sol. Energy 76 (2004) 255–262, https://doi.org/10.1016/j.solener.2003.07.033.
[27] S. Wang, D. MacDonald, Temperature dependence of Auger recombination in highly injected crystalline silicon, J. Appl. Phys. 112 (2012), https://doi.org/10.1063/1.4768900.
[28] P.P. Altermatt, F. Geelhaar, T. Trupke, X. Dai, A. Neisser, E. Daub, Injection dependence of spontaneous radiative recombination in c-Si: experiment theoretical analysis and simulation, Proc. 5th Int. Conf. Numer. Simul. Optoelectron. Dev. (2005) 47–48, https://doi.org/10.1109/NUSOD.2005.1518128.
[29] F. Kersten, P. Engelhart, H.C. Ploigt, A. Stekolnikov, T. Lindner, F. Stenzel, M. Bartzsch, A. Szpeth, K. Petter, J. Heitmann, J.W. Müller, Degradation of multicrystalline silicon solar cells and modules after illumination at elevated temperature, Sol. Energy Mater. Sol. Cells 142 (2015) 83–86, https://doi.org/10.1016/j.solmat.2015.06.015.
[30] R. Eberle, W. Kwapil, F. Schindler, M.C. Schubert, S.W. Glunz, Impact of the firing temperature profile on light induced degradation of multicrystalline silicon, Phys. Status Solidi Rapid Res. Lett. 10 (2016) 861–865, https://doi.org/10.1002/pssr.201600272.
[31] M.A. Jensen, A.E. Morishige, S. Chakraborty, R. Sharma, H.S. Laine, B. Lai, V. Rose, A. Youssef, E.E. Looney, S. Wieghold, J.R. Poindexter, J.P. Correa-Baena, T. Felisca, H. Savin, J.B. Li, T. Buonassisi, Solubility and diffusivity: important metrics in the search for the root cause of light-and elevated temperature-induced degradation, IEEE J. Photovolt. 8 (2018) 448–455, https://doi.org/10.1109/JPHOTOV.2018.2791411.
[32] H. Vahlman, A. Haarahiltunen, W. Kwapil, J. Schön, A. Inglese, H. Savin, Modeling of light-induced degradation due to Cu precipitation in p-type silicon. II. Comparison of simulations and experiments, J. Appl. Phys. 121 (2017), https://doi.org/10.1063/1.4983455.